Original Paper

Cellular Physiology and Biochemistry

Cell Physiol Biochem 2011;28:1031-1044

Accepted: October 25, 2011

Regulation of Myosin Light Chain Function by BMP Signaling Controls Actin Cytoskeleton Remodeling

Georgios Konstantinidis[1], Aristidis Moustakas[2,3] and Christos Stournaras[1]

[1]Department of Biochemistry, University of Crete Medical School, Heraklion, [2]Ludwig Institute for Cancer Research, Uppsala University, Biomedical Center, Uppsala, [3]Department of Medical Biochemistry and Microbiology, Science for Life Laboratory, Uppsala University, Uppsala

Key Words

Actin • Bone morphogenetic protein • Cytoskeleton • Myosin light chain • Myosin light chain kinase • Rho coiled-coiled kinase 1 • Transforming growth factor β

Abstract

Background/Aims: Actin cytoskeleton dynamics support and coordinate signaling events that control cell proliferation, differentiation and migration. Growth factors provide essential signals that act on multi-protein complexes that regulate actin assembly with myosin. We previously analyzed the action of the transforming growth factor β (TGF-β) and now extend our studies to the bone morphogenetic protein (BMP) 7, an important regulator of stem cell function and bone differentiation. Methods: Using a well-established cell model of actin dynamics, Swiss3T3 fibroblasts, we applied cell biological and biochemical approaches to monitor the pathway that links the BMP-7 receptors to the acto-myosin complex. Results: We demonstrate that BMP-7 induces actin and focal adhesion remodeling in starved fibroblasts as potently as TGF-β. BMP-7 mediates changes of actin dynamics via the kinase ROCK1 and induces rapid activation of RhoA and RhoB with concomitant inactivation of Cdc42. These molecular events correlate well with induction of phosphorylation on Ser19 of the myosin light chain, but not with LIMK1 kinase activation. Depletion of endogenous myosin light chain inhibits actin remodeling induced by BMP-7. This novel pathway regulates fibroblast migration without affecting cell proliferation. Conclusion: We establish a BMP-Rho-ROCK1 pathway, which targets myosin light chain to control actin remodeling in fibroblasts.

Introduction

Signal transduction pathways control the local and global architecture of actin microfilaments, which is a critical process supporting cellular morphogenesis and differentiation, proliferation, motility and secretion [1, 2]. In many cell types, signaling by various cytokines initiates a rapid reorganization of the actin cytoskeleton. Small GTPases of the Rho family play critical roles in transmitting the signals that target dynamic changes of the actin microfilament [3]. In a well-established signaling

KARGER

Fax +41 61 306 12 34
E-Mail karger@karger.ch
www.karger.com

1015-8987/11/0285-1031$38.00/0

Accessible online at:
www.karger.com/cpb

C. Stournaras
Department of Biochemistry, University of Crete Medical School
Heraklion, GR-71110 (Greece), E-Mail cstourn@med.uoc.gr
or A. Moustakas, Ludwig Institute for Cancer Research
Box 595, SE-751 24 Uppsala (Sweden), E-Mail aris.moustakas@licr.uu.se

scenario, signaling receptors from the plasma membrane induce phosphorylation of guanine exchange factors, which results in the loading of a Rho family GTPase with GTP, thus locking the enzyme in its active form [4]. The activated Rho GTPase induces the kinase activity of the Rho coiled-coiled kinase 1 (ROCK1) [5] or alternatively can induce the p21-activated kinase 1 (PAK1) [6]. Downstream of the PAK1 and ROCK1 kinases act the related kinases LIM-kinase 1 and 2 (LIMK1 and LIMK2), which can be directly phosphorylated by their upstream regulators respectively [7]. A critical target of the LIMKs is cofilin, which is inactivated after phosphorylation, a condition required for actin polymerization to occur [8, 9]. The functional impact of the actin microfilament network on cell motility is controlled by its association with the myosin chain and regulatory enzymes that control the activity of myosin, such as myosin light chain kinases [10]. In summary, a coordinated cascade of GTPase and kinase activities control the assembly and contractility of the acto-myosin filaments in non-muscle cells, ensuring proper motility under the guidance of growth factors.

The transforming growth factor β (TGF-β) family of cytokines plays major roles in many different cellular processes, including proliferation, cell apoptosis, immune response and differentiation [11]. This family includes several cytokines, including bone morphogenetic proteins (BMPs) and activins. Misregulation of signaling in this family is involved in several diseases, including cancer [12, 13]. Like other ligands in the TGF-β family, the BMPs signal through binding to two types of transmembrane serine/threonine kinase receptors. Ligand binding allows the constitutively active type II receptor to phosphorylate the type I receptor at its Gly-Ser juxtamembrane domain, thus activating the kinase activity of the type I receptor [14]. Activated BMP type I receptors phosphorylate receptor-regulated Smads (R- Smads), Smad1, Smad5 and Smad8 at the carboxy-terminal Ser-X-Ser motifs where after they form complexes with the common-mediator Smad (Co-Smad; Smad4) [14]. Together with Smad4, Smad1/5/8 accumulate in the nucleus and bind to the promoters of target genes to regulate their transcription. In addition to Smad signaling, the BMP receptors activate other signaling effectors such as TAK1 (TGFβ-activated kinase 1), p38 MAP kinase and JNK (c-Jun N-terminal kinase) [15].

The control of cell motility by TGF-β is important during wound healing and cancer cell invasiveness [16, 17]. An important mechanism that mediates motility changes by TGF-β is the regulation of the actin cytoskeleton by TGF-β, a process that is currently understood in good detail [16, 18]. However, the role of BMP signaling in mediating changes on the actin cytoskeleton and acto-myosin contractility remains less explored [16]. A signaling pathway has been studied in pulmonary cells and during dendritogenesis of neurons, whereby the long cytoplasmic tail of the BMP type II receptor binds directly to LIMK1 and sequesters it from regulating cofilin [19, 20]. Upon BMP signaling, LIMK1 dissociates from the BMP receptor and phosphorylates cofilin, thus affecting actin polymerization. During dendrite formation, the BMP type II receptor also binds to the c-Jun N-terminal kinase, which mediates the stabilization of microtubules, an event required for dendritogenesis concomitant to the actin remodeling [21]. A BMP receptor-LIMK1-microtubule (but not actin) pathway has also been delineated during neuronal synaptic stabilization in *Drosophila* [22], while in *Xenopus* retinal ganglia, LIMK1 was shown to be activated by the BMP type II receptor in axons but not dendrites [23]. These studies suggest a complexity and cell-type or species specificity of the BMP-LIMK1 pathway. In C2C12 myoblasts that undergo differentiation into osteoblasts in response to BMPs but also exhibit enhanced motility, BMP-2 was shown to initiate signaling via the Cdc42 small GTPase and the phosphoinositide-3′-kinase, which affected the activation of several PAK isoforms and LIMK1 [24]. This pathway had a critical impact on the actin cytoskeleton reorganization induced by BMP-2 in the motile myoblasts.

We have previously shown that TGF-β signals in Swiss3T3 fibroblasts via its canonical type I receptor to elicit activation of RhoA and RhoB, and subsequent phosphorylation of LIMK2 and cofilin, as critical events during reorganization of the actin cytoskeleton [25]. We have now expanded this work to the BMP signaling system and demonstrate that similar to TGF-β, BMP-7 induces activation of RhoA and RhoB, however, this correlates with phosphorylation of ROCK1 and not of LIMK1/2. A consequence of this new pathway is the regulation of the myosin light chain (MLC) during BMP-induced remodeling of the actin network.

Materials and Methods

Reagents and transfections

Mouse Swiss3T3 and NIH3T3 fibroblasts were obtained from the American Type Culture Collection. Recombinant mature human TGF-β1 was from R&D Systems Inc., and mature recombinant BMP-7 was a gift from K. Sampath (Curis Inc.). ROCK inhibitor Y-27632 and MLCK inhibitor ML-7 were from

Sigma. RT-PCR primers for RhoA, RhoB and Gapdh transcripts (Table 1) were from the Microchemistry lab, IMBB, FORTH (kindly provided by Dr. D. Kardassis). Mouse MLC-specific siRNA, 5'-GAGAAGGGCAGGAGCG GÁÁ-3'(sense strand) corresponding to nucleotides 114-133 (Genbank ID: NM_016754), by numbering as nucleotide 1 the A of the ATG translational start codon was from Eurofins MWG Operon. The Silencer negative control siRNA was from Ambion. Transient transfection of NIH3T3 cells in 6-well plates using 1.33 μg siMLC or Silencer negative control and 5 μL Lipofectamine 2000 transfection reagent (Invitrogen) per well was performed according to the manufacturer's instructions.

Direct Actin Fluorescence and Immunofluorescence Microscopy

Swiss3T3 cell monolayers were serum-starved for 24 h and then treated with 5 ng/mL TGF- β1 or 30 ng/mL BMP-7; alternatively, cells were pretreated for 45 min with ROCK and MLCK inhibitors (10 μM Y-27632 and 5 μM ML-7 respectively) and then treated with 30 ng/mL BMP-7 as indicated in the corresponding figure legends. Cells were prepared as previously described [25]. Rhodamine-phalloidin was from Molecular Probes, Inc. (1:100 dilution); mouse monoclonal anti-vinculin (Clone VIN-11-5 1:500 dilution) was from Sigma-Aldrich; FITC-conjugated rabbit anti-mouse IgG (1:200 dilution) was from Chemicon. Slides were mounted using ProLong® Gold antifade reagent with DAPI (Invitrogen). Photomicrographs were obtained with a Leica DMLB microscope equipped with fluorescence illumination and photographed with Leica DC 300F camera, using the Leica Germany 40/0.75 HCX PL FLUOTAR objective lens and photographing at ambient temperature in the absence of immersion oil. Images were acquired with the camera's Leica IM 50 software and, using the Adobe Photoshop software, image memory content was reduced and brightness-contrast was adjusted.

Immunoblotting Analysis

Total protein extracts were analyzed by sodium dodecyl sulfate/polyacrylamide gel electrophoresis/Western blotting as described previously [25]. For immunodetection, mouse monoclonal anti-RhoA (26C4, 1:100 dilution), rabbit polyclonal anti-RhoB (119, 1:100 dilution), mouse monoclonal anti-Cdc42 (B-8, 1:100 dilution), rabbit anti-pLIMK1/2 (Thr508/505 1:100 dilution), goat anti-LIMK1 (C-18 1:100 dilution), were purchased from Santa Cruz Biotechnology, Inc., mouse anti-myosin (light chains) (clone MY-21 1:200 dilution) from Sigma-Aldrich, rabbit anti-phospho-p38 (Thr180/Tyr182 1:2000 dilution), rabbit anti-p38 (1:2,000 dilution), rabbit anti-phospo-p44/p42 MAPK (Erk1/2) (Thr202/Tyr204 1:2,000 dilution), rabbit anti-p44/p42 MAPK (Erk1/2) (1:2,000 dilution), rabbit anti-phospho-Myosin Light Chain 2 (Ser19 1:100 dilution) from Cell Signaling Technology, mouse anti-actin (Clone C4 1:1,000 dilution) from Chemicon International, rabbit anti-Smad1 (1:1,000 dilution) from Epitomics and rabbit anti-phospho-Smad1 (1:1,000 dilution) was produced in house (Ludwig Institute for Cancer Research). Secondary anti-mouse-IgG and anti-rabbit-IgG coupled to horseradish peroxidase were from Amersham Biosciences (1:10,000 dilution).

Primer	Sequence
mRhoA sense	5′ CCAGACTAGATGTAGTATTTTTTG 3′
mRhoA antisense	5′ GAGCCAGACCCTGCAGTCCAG 3′
mRhoB sense	5′ CCCACCGTCTTCGAGAACTA 3′
mRhoB antisense	5′ CTTCCTTGGTCTTGGCAGAG 3′
GAPDH forward	5′ ACCACAGTCCATGCCATCAC 3′
GAPDH reverse	5′ TCCACCACCCTGTTGCTGTA 3′

Table 1. Primers that were used to amplify the transcripts of RhoA, RhoB, Smad6 and Gapdh genes.

Anti-goat-IgG coupled to horseradish peroxidase was from Santa Cruz Biotechnology, Inc. (1:8,000 dilution). The enhanced chemiluminescence detection system was purchased from Amersham Biosciences. Protein band intensity was quantified using the Tina Scan v.2 software for image analysis. For biochemical determination of the ratio of soluble actin to total actin after desired stimulation as indicated in the corresponding figure legends, Swiss3T3 cells were incubated for 5 min in 0.3% Triton-X-100 lysis buffer (5 mM Tris, 2 mM EGTA, 300 mM sucrose, 400 μM phenylmethylsulfonylfluoride, 10 μM leupeptin, 2 μM phalloidin) and precipitated with equal volume of 6% perchloric acid [Total soluble cluster (Ts)]. Insoluble proteins were scraped and precipitated with 3% perchloric acid [Total insoluble cluster (Ti)]. Pellets were diluted in 0.1 M NaOH. Equal volumes of Ts and Ti clusters mixed with 2x sample buffer were analyzed by sodium dodecyl sulfate/polyacrylamide gel electrophoresis/Western blotting and band intensity of Ts cluster were divided with the sum (total) of the band intensity of Ts and Ti cluster.

Rho-GTP assay

For affinity precipitation with Rhotekin-RBD Protein GST Beads and PAK-GST Protein Beads (Cytoskeleton), Swiss3T3 cells were serum-starved for 24 h and then stimulated with 30 ng/mL BMP-7 as indicated in the corresponding figure legend. The cells were then washed with ice-cold Tris-buffered saline and lysed with cell lysis buffer (50 mM Tris pH 7.5, 10 mM $MgCl_2$, 0.3 M NaCl, 2% IGEPAL ((Octylphenoxy)-polyethoxyethanol), 10 μg/mL aprotinin, 10 μg/mL leupeptin, 1 mM phenylmethylsulfonyl fluoride, 25 mM NaF, 1 mM Na_3VO_4 and 1 mM dithiolthreitol). Cleared cell lysates were incubated with 60 μg of Rhotekin-RBD Protein GST (glutathione S-transferase) beads for RhoA and RhoB and 20 μg PAK-GST Protein beads for Cdc42 at 4°C for 1 h and washed with wash buffer (25 mM Tris pH 7.5, 30 mM $MgCl_2$, 40 mM NaCl, 10 μg/mL aprotinin, 10 μg/mL leupeptin, 1 mM phenylmethylsulfonyl fluoride, 25 mM NaF, 1 mM Na_3VO_4 and 1 mM DTT). GTP-bound Rho was detected by immunoblotting using the appropriate antibody. Protein band intensity was quantified using the Tina Scan v.2 software.

In Vitro Kinase Assay

Swiss3T3 cells were serum-starved for 24 h then treated or not with 10 μM Y-27632 for 45 min and stimulated with 30 ng/mL BMP-7 for the time periods indicated in the corresponding figure legend. Then cells were washed with ice-cold Tris-buffered saline, suspended in lysis buffer (50 mM Tris pH 7.5, 1% Triton X-100, 500 mM NaCl, 10 mM NaF, 10% glycerol, 25 mM glycerophosphate, 1 mM Na_3VO_4, 1 mM phenylmethyl-sulfonyl fluoride, 2 μg/ml aprotinin, 2 μg/ml leupeptin) and incubated on ice for 30 min. Cleared lysates were pre- adsorbed to A-protein-agarose beads (Santa Cruz Biotechnology, Inc.) for 1 h at 4°C and centrifuged, the supernatants (equal amounts of protein) were subjected to immunoprecipitation using the goat anti-LIMK1 antibody described above and protein A- Agarose beads. Immunoprecipitated LIMK1 beads were washed three times with kinase buffer (50 mM Hepes/NaOH pH 7.5, 25 mM β-glycerophosphate, 5 mM $MgCl_2$, 5 mM $MnCl_2$, 10 mM NaF, 1 mM Na_3VO_4) and incubated for 30 min at 30°C in 20 μl of the kinase buffer containing 15 μM ATP and 5 μCi of [^{32}P] ATP (5,000 Ci/mmol, Amersham Biosciences). Proteins were resolved by 11% polyacrylamide gel electrophoresis (0.4% w/v sodium dodecyl sulfate), transferred onto nitrocellulose, and ^{32}P-labeled proteins were visualized by autoradiography on X-ray films.

Migration and Proliferation Assays

Wound healing. 100% confluent Swiss3T3 cells were serum-starved for 24 h, then treated or not with 10 μM Y-27632 for 45 min, scratched and stimulated with 30 ng/mL BMP-7 for 24 h. Photomicrographs were obtained as described at Immuno-fluorescence Analysis and as indicated in the corresponding figure legend.

MTT assay. 12,000 Swiss3T3 cells per well of 96-well plate were serum-starved for 24 h, stimulated with 30 ng/mL BMP-7 for 20 h, and incubated with 0.25 mg/mL tetrazolium for 4 h. Then, insoluble purple formazan crystals were solubilized by the addition of 200 μL DMSO and color quantified by Model 680 Microplate Reader (Bio-Rad Laboratories (UK) Ltd) using measurement filter at 550 nm and reference filter at 655 nm.

RT-PCR assay. Swiss3T3 cells were serum-starved for 24 h then stimulated with 30 ng/mL BMP-7 as indicated in the corresponding figure legend. Cell lysates were processed for total RNA extraction using Trizol reagent (Applied Biosystems) according to the manufacturer's instructions. The first cDNA strand was synthesized using Superscript II Rnase H-reverse transcriptase (Invitrogen). Amplification of mouse RhoA and RhoB cDNA were performed using the primers indicated in the Table 1. Normalization of cDNA production was performed by amplifying the mouse housekeeping glyceraldehyde-3'-phosphate dehydrogenase (Gapdh) gene. The quantification of the results was performed by measuring the intensity of the bands using the Tina Scan v.2 software.

Statistical analysis

Quantitative experimental data derived from actin solubility assays, proliferation assays and RT-PCR assays were analyzed statistically based on a standard two-tailed t-test for samples with unequal variance. Significance is indicated with p values as reported in the figure legends.

Results

BMP-7 induces rapid and sustained reorganization of the actin cytoskeleton

We previously delineated a mechanism that controls actin cytoskeleton reorganization downstream of TGF-β in Swiss3T3 fibroblasts [25]. We then asked whether the same or a distinct molecular pathway could regulate actin dynamics downstream of the related cytokine BMP-7. Time course experiments where TGF-β1 and BMP-7 were compared side-by-side revealed that BMP-7 was equally potent as TGF-β1 in inducing rapid, robust and sustained actin reorganization in serum-starved Swiss3T3 cells (Fig. 1A). The architectural effect on actin micro-filaments was quantified by measuring the Triton-X-100-soluble (Ts) and insoluble (Ti) levels of actin from the cells using quantitative immunoblotting [26]. As expressed in the sets of Fig. 1A and graphed in Fig. 1B, TGF-β1 induced a gradual reduction in the Ts/Total actin ratio, which is equivalent to an increase in polymerized (insoluble) actin, while BMP-7 induced a more rapid induction in actin polymerization that sustained for up to 24 h post-stimulation.

Actin reorganization is usually associated with formation of focal adhesions at the plasma membrane. We therefore co-stained the stimulated cells for polymerized actin and vinculin, a central component of focal adhesions (Fig. 2). BMP-7 potently induced large numbers of brightly stained focal adhesions localizing at the tips of actin stress fibers, similar to TGF-β1. We therefore conclude that BMP-7 signaling is equipotent to TGF-β signaling in mediating actin reorganization in fibroblasts.

BMP-7 promotes cell migration without affecting cell proliferation

A strong physiological corollary of dynamic actin reorganization in response to growth factor signaling often is cell migration. We measured Swiss3T3 cell migration using a wound healing assay (Fig. 3A). Cells slowly migrated into the wound over the course of 24 h under serum starvation conditions. Upon stimulation with BMP-7, cell migration was significantly accelerated as visualized by the degree of wound closure (Fig. 3A). This finding agrees with the observed actin reorganization occurring in the cells during the same time interval of 24 h.

Wound healing assays often measure the combined ability of cells to migrate and proliferate. For this reason we also measured the potential of BMP-7 in

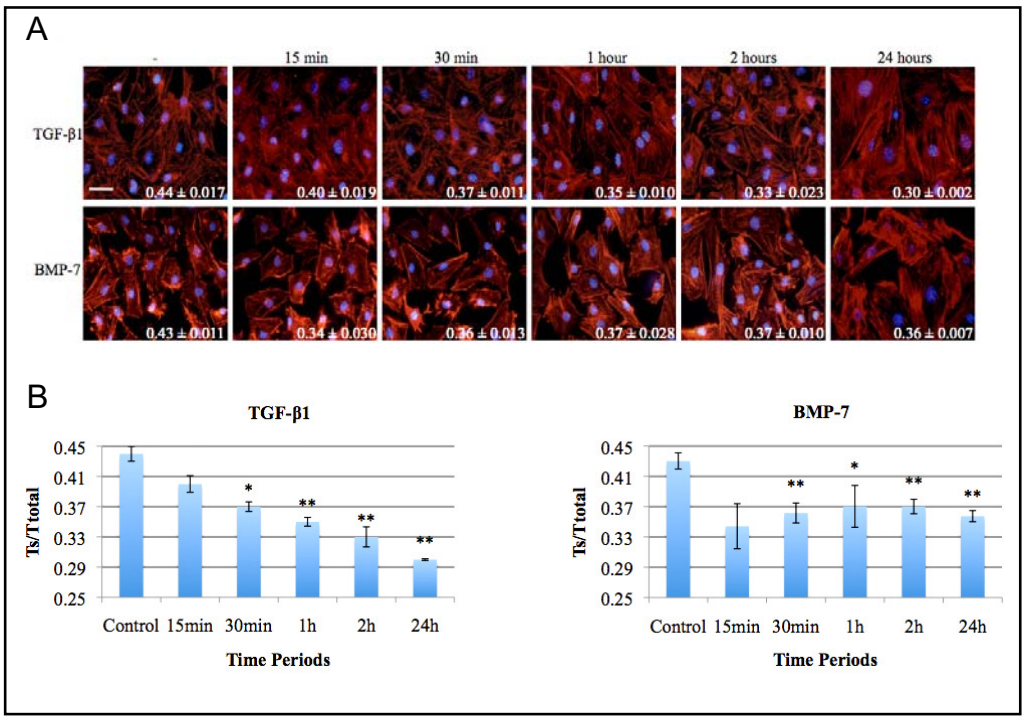

Fig. 1. TGF-β1 and BMP-7 induce rapid and sustained reorganization of actin cytoskeleton in Swiss3T3 fibroblasts. A. Swiss3T3 fibroblasts serum-starved for 24 h were stimulated with 5 ng/mL TGF-β1 or 30 ng/mL BMP-7 for the indicated time periods. Cells were then fixed and direct fluorescence labeling with rhodamine-phalloidin and DAPI was carried out. A bar represents 10 μm. B. The ratios presented in bar graphs are showing mean values ± S.E. of Ts/Total of three distinct experiments (*, $p<0.05$ and **, $p<0.01$). The same ratios are also indicated within the microphotographs (low right corner).

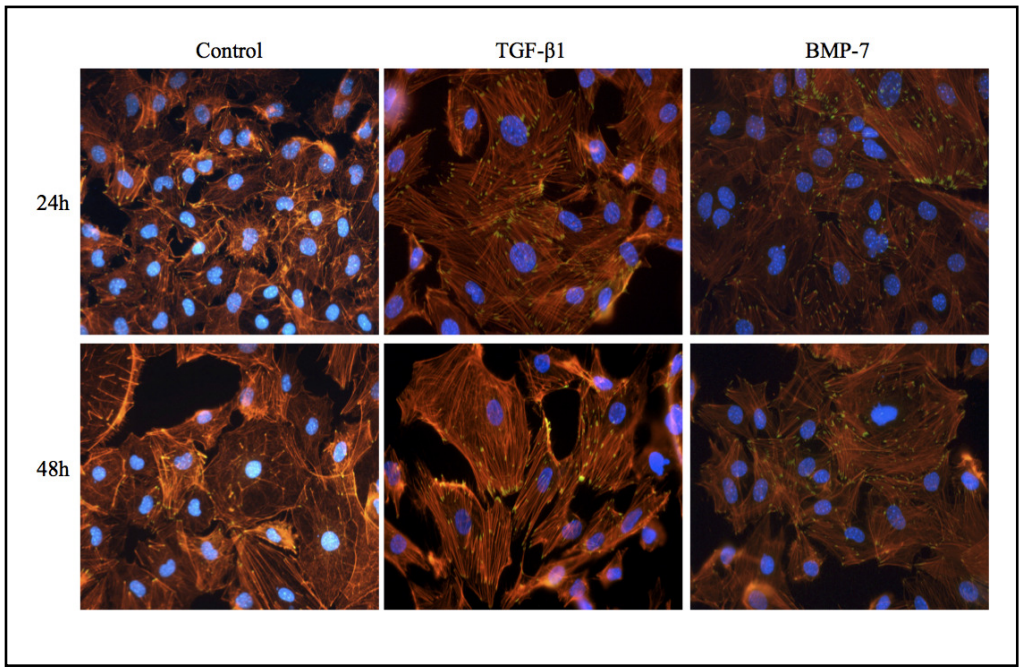

Fig. 2. TGF-β1 and BMP-7 affect the distribution of vinculin in Swiss3T3 fibroblasts. Swiss3T3 fibroblasts were serum-starved for 24 h, then stimulated for 24 h and 48 h with 5 ng/mL TGF-β1 or 30 ng/mL BMP-7. Cells were then fixed and direct fluorescence labeling with rhodamine-phalloidin (red) and DAPI (blue) and immunofluorescence labeling with anti-vinculin (green) was carried out. There is extensive localization of vinculin at the ends of actin filaments (yellow spots) after 24 h and 48 h TGF-β1 and BMP-7 stimulation. A bar represents 20 μm.

modulating cell proliferation under the same conditions (Fig. 3B). In the Swiss3T3 system, while TGF-β1 could potently stimulate cell proliferation as established before (and here used as positive control), BMP-7 failed to score significantly in any of the proliferation assays performed. These data suggest that BMP-7 stimulates a genuine actin reorganization that correlates with cell migration but not with any significant proliferative response of the target cells.

BMP-7 induces Smad1, MAPK and Rho GTPase signaling

In order to investigate the mechanism by which BMP-7 elicited its effects on the actin cytoskeleton, we assayed for a number of signaling proteins that are known to act downstream of the BMP receptors. Namely we focused on Smad1, the major Smad protein signaling downstream of BMP receptors, and on the mitogen activated protein kinases (MAPK) p38 and Erk1/2, which

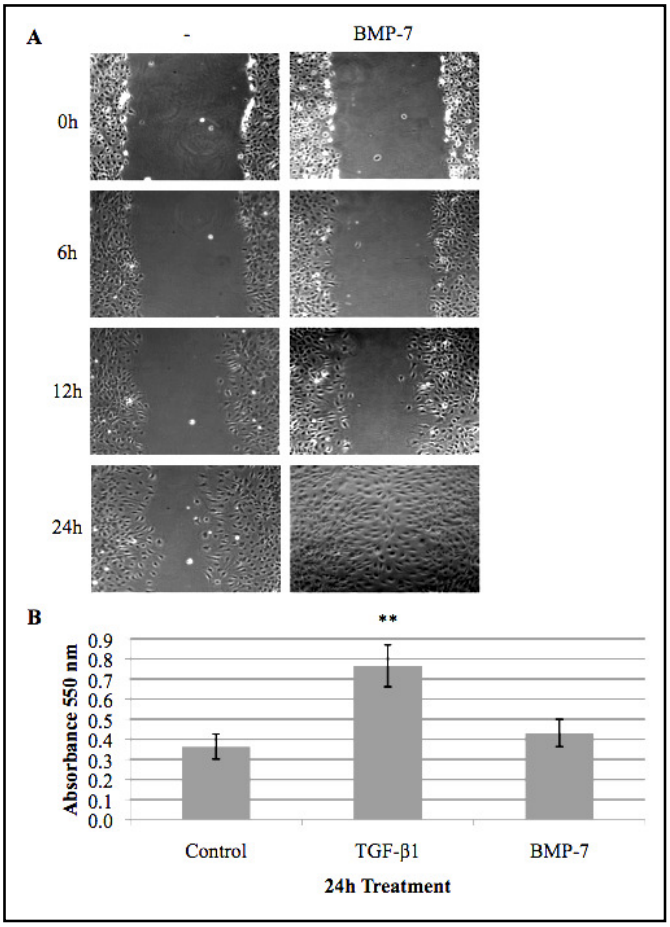

Fig. 3. Regulation of cell migration and proliferation. A. BMP-7 induces migration in Swiss3T3 fibroblasts. 100% confluent Swiss3T3 fibroblasts serum-starved for 24 h scratched and stimulated with 30 ng/mL BMP-7 for 24 h showed induced migration activity. A bar represents 25 μm. B. BMP-7 does not induce proliferation in Swiss3T3 fibroblasts. Swiss3T3 fibroblasts serum-starved for 24 h were stimulated with 5 ng/mL TGF-β1 and 30 ng/mL BMP-7 for 20 h. Then cells were incubated for 4 h with MTT reagent and the color intensity was recorded on a plate reader. TGF-β1 treatment induces proliferation of Swiss3T3 fibroblasts, however BMP-7 has a more moderate effect in proliferation. The bar graphs are showing mean values ± S.E. of fold increase proliferation of six distinct experiments (**, $p<0.01$).

are also well-established as signaling downstream of BMP [15]. Finally, we also assayed the impact of BMP-7 on the activation of Rho GTPases as these enzymes are the best upstream regulators of dynamic actin reorganization in various cell systems [3, 18].

Analysis of the events occurring during the first 4 h after BMP-7 stimulation revealed immediate-early, robust and sustained induction of phospho-Smad1 levels (Fig. 4A). The antibody used recognizes phosphorylation of the two C-terminal serine residues of Smad1 that are directly phosphorylated by the BMP type I receptor, and serves as measurement of direct receptor signaling activity. Peak levels of phospho-Smad1 were achieved as early as 15 min post-stimulation with BMP-7 in this cell system. BMP-7 stimulation did not appreciably affect the total levels of Smad1 protein as expected (Fig. 4A).

BMP-7 also induced the phosphorylation of p38 MAPK with a peak of phosphorylated levels at 1 h post-stimulation (Fig. 4A). In contrast, the phosphorylated Erk1/2 levels were high in Swiss3T3 cells, despite the starvation from serum and BMP-7 did not appreciably affect those at the immediate-early time periods (30 min), however, the levels of phospho-Erk1/2 decreased gradually after 1 h of stimulation, whereas the total levels of Erk1/2 proteins remained constant (Fig. 4A). We conclude that the time-dependent effects of BMP-7 on actin reorganization best correlate with the activation of Smad1 and also possibly with the activation of p38 MAPK and deactivation of Erk1/2 MAPKs in Swiss3T3 cells.

In addition to Smad1 and p38 MAPK, BMP-7 stimulation gave rise to immediate-early and robust levels of GTP-loaded RhoA and RhoB (Fig. 4B). The elevated levels of RhoA-GTP were evident within 15 min, remained up to 1 h post-stimulation and then gradually decreased. Interestingly, RhoB-GTP activation remained almost unchanged during short-term BMP-7 stimulation then it was clearly elevated within 2 h post-stimulation and remained active for at least up to 4 h. In contrast, the related small GTPase Cdc42 exhibited strong GTP-loaded levels in control serum-starved and not-stimulated cells, which were rapidly reduced in response to BMP-7 (Fig. 4B).

We have recently described a transcriptional mechanism based on which TGF-β signaling, via Smads induces expression of the RhoB, but not of the RhoA, gene [27, 28]. We were therefore interested in testing whether BMP-7 could affect in a similar manner expression of RhoA or RhoB mRNA. RT-PCR assays demonstrated that indeed BMP-7 could induce reproducible, albeit weak levels of RhoB mRNA during the early phase (1-4 h) of the time course (Fig. 4C). In contrast, BMP-7 had no effect on RhoA gene expression. The induction of RhoB mRNA by BMP-7 was weaker than that recorded after TGF-β1 stimulation [28], and also significantly weaker than the induction of a well-established target gene of BMP signaling [29], the inhibitory Smad6 (Fig. 4D). Finally, the total protein levels of RhoB did not change appreciably during the 4-hour time course (Fig. 4B), suggesting that the weak regulation

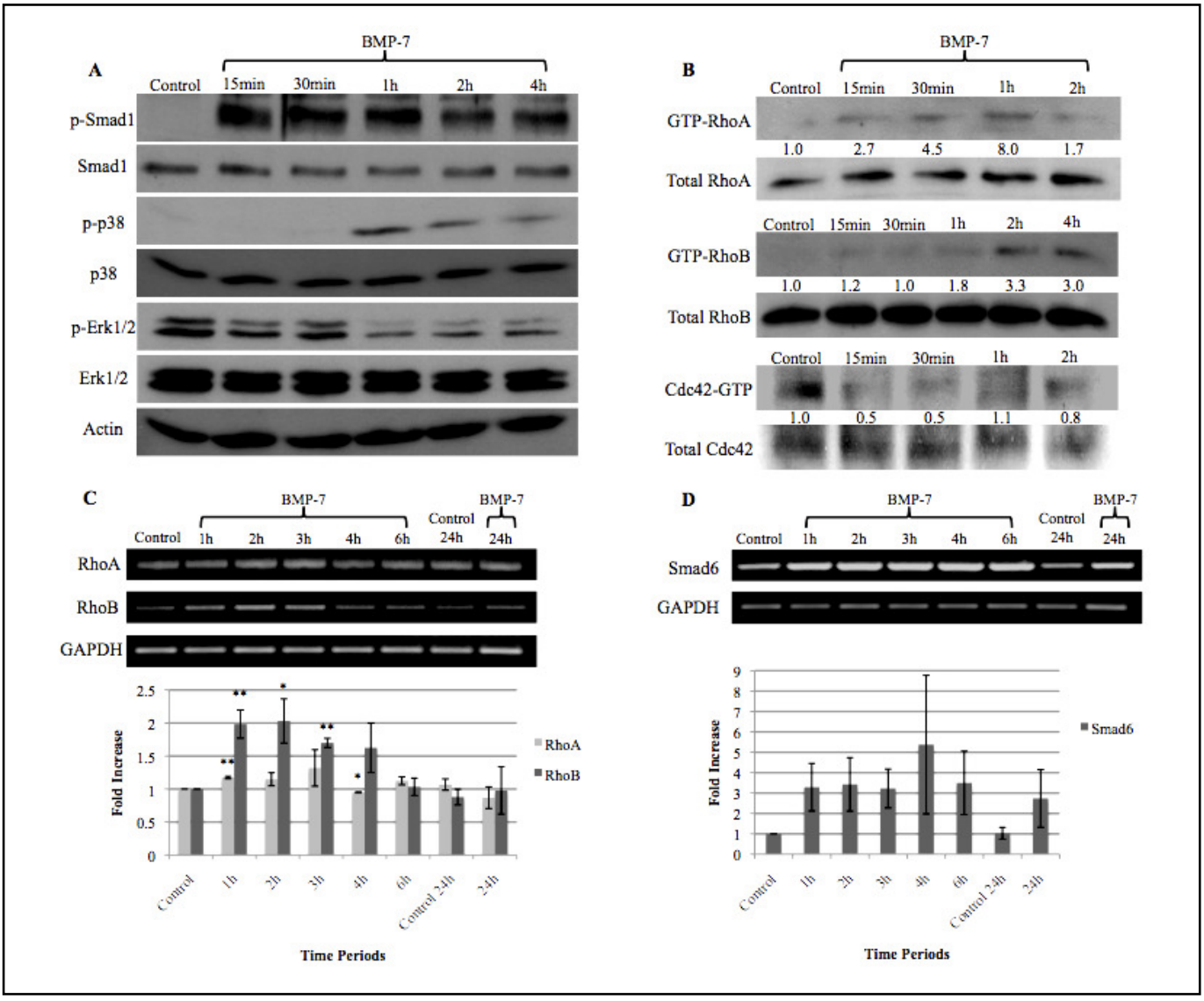

Fig. 4. Signaling pathways and gene regulation induced by BMP-7. A. BMP-7 affects the phosphorylation of Smad1 and MAPK in Swiss3T3 fibroblasts. Representative blots are showing the amount of Smad1, p38 and p44/p42 MAPK (Erk1/2) phosphorylation from 24 h-serum-starved non-stimulated (Control) and BMP-7-stimulated (30 ng/mL) Swiss3T3 fibroblasts for the indicated time periods. B. BMP-7 induces rapid GTP loading of RhoA and RhoB and GTP loss of Cdc42. Representative blots are showing the amount of active GTP-bound RhoA, RhoB and Cdc42, determined by a GST pull-down assay, from 24 h-serum-starved non-stimulated (Control) or BMP-7-stimulated (30 ng/mL) Swiss3T3 fibroblasts for the indicated time periods. BMP-7 stimulation for 15 min led to GTP loading of RhoA and RhoB. The most extensive GTP-loading occurs at 1 h of BMP-7 stimulation for RhoA and at 2 and 4 h for RhoB. Interestingly, there is GTP loss of Cdc42 at 15 and 30 min of BMP-7 stimulation. Numerical values between the immunoblots indicate densitometric fold change measurements of GTP-loaded band intensity normalized to the corresponding total protein band intensity. C and D. Representative RT-PCR experiments showing the amount of mRNA levels of RhoA, RhoB and Smad6 from non-stimulated (Control) and BMP-7-stimulated (30 ng/mL) Swiss3T3 fibroblasts for the indicated time periods. The ratios of band intensity of the specific cDNA normalized to the Gapdh cDNA are presented in bar graphs as mean values ± S.E. of the expressed RhoA, RhoB and Smad6 of three distinct experiments (*, $p<0.05$ and **, $p<0.01$) and are shown below each set of DNA gels. Although BMP-7 does not induce significant increase of RhoA mRNA levels, it does induce increased mRNA levels of RhoB (1-4 h treatment) and Smad6 (1-24 h treatment).

at the mRNA level may not be translated at the protein level.

We conclude that BMP-7 initiates a signaling pathway that involves both Smad1 and p38 MAPK. In addition, it induces robust RhoA-GTP levels, which cannot be mediated via a transcriptional mechanism mediated by the Smad pathway. It is assumed that early RhoA activation by BMP-7 controls mainly the early actin

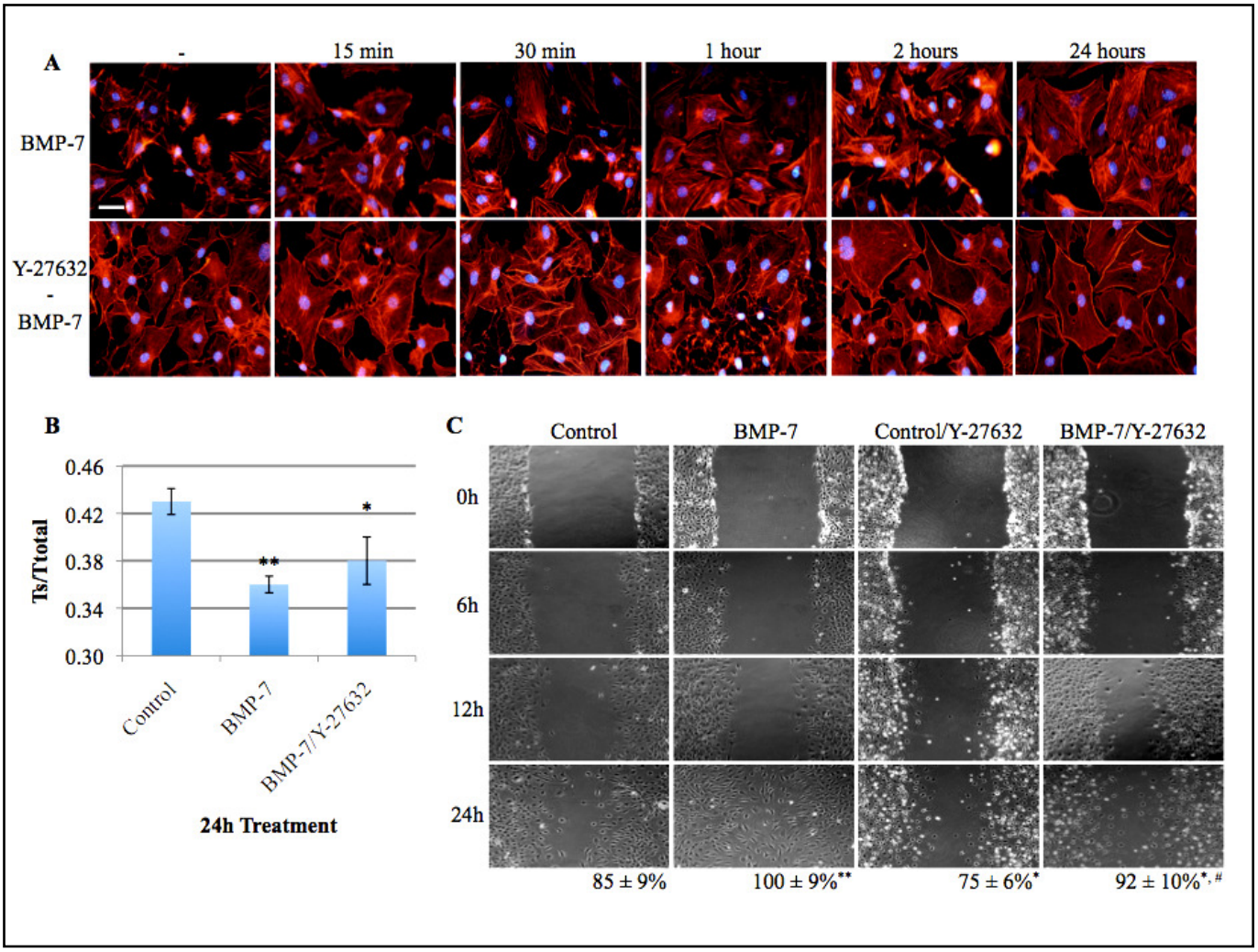

Fig. 5. The ROCK inhibitor Y-27632 blocks BMP-7-mediated actin reorganization. A. Swiss3T3 fibroblasts serum-starved for 24 h were stimulated with 30 ng/mL BMP-7 for the indicated time periods after pretreatment with 10 μM Y-27632 for 45 min. Cells were fixed and stained with rhodamine-phalloidin and DAPI. A bar represents 10 μm. B. The ratios presented in bar graphs are showing mean values ± S.E. of Ts/Total of three distinct experiments of BMP-7-stimulated (30 ng/mL) Swiss3T3 fibroblasts for 24 h (*, $p<0.05$ and **, $p<0.01$). C. The ROCK inhibitor Y-27632 affects BMP-7-induced migration in Swiss3T3 fibroblasts. 100% confluent Swiss3T3 fibroblasts serum-starved for 24 h were scratched and then were stimulated with 30 ng/mL BMP-7 for 24 h after pretreatment with 10 μM Y-27632 for 45 min. Photos were taken for the indicated time periods. Y-27632-treated cells show much lower density at the healed area of the wound. The percentages under the low right corner of last line of the microphotographs are showing mean values ± S.E. of the wound closure of three distinct experiments. (*, $p<0.05$ and **, $p<0.01$). #represents the statistical analysis comparison between BMP-7 and BMP-7/Y-27632-induced closure of the wound (#, $p<0.05$). A bar represents 25 μm.

reorganization. In parallel, RhoB-GTP activation may govern the long-term actin reorganization events. These findings corroborate the RhoA/B GTPase activation profile shown in Fig. 4B.

The kinase ROCK1 mediates actin reorganization downstream of BMP-7

GTP-loaded RhoA is best known to induce the enzymatic activity of the kinase ROCK1 [3]. We therefore reasoned that if BMP-7 had an immediate impact on RhoA-GTP levels, which had functional significance, then interfering with the activity of the ROCK1 kinase should block the effects of BMP-7 on the cytoskeleton.

Indeed co-treatment of serum-starved cells with BMP-7 and the ROCK1 low molecular weight inhibitor Y-26763, completely blocked the potential for central actin stress fiber formation (Fig. 5A) while the peripheral actin structures remained unaffected. This is in line with previously reported effects of Y-26763 on the actin cytoskeleton of human foreskin fibroblasts [30]. The

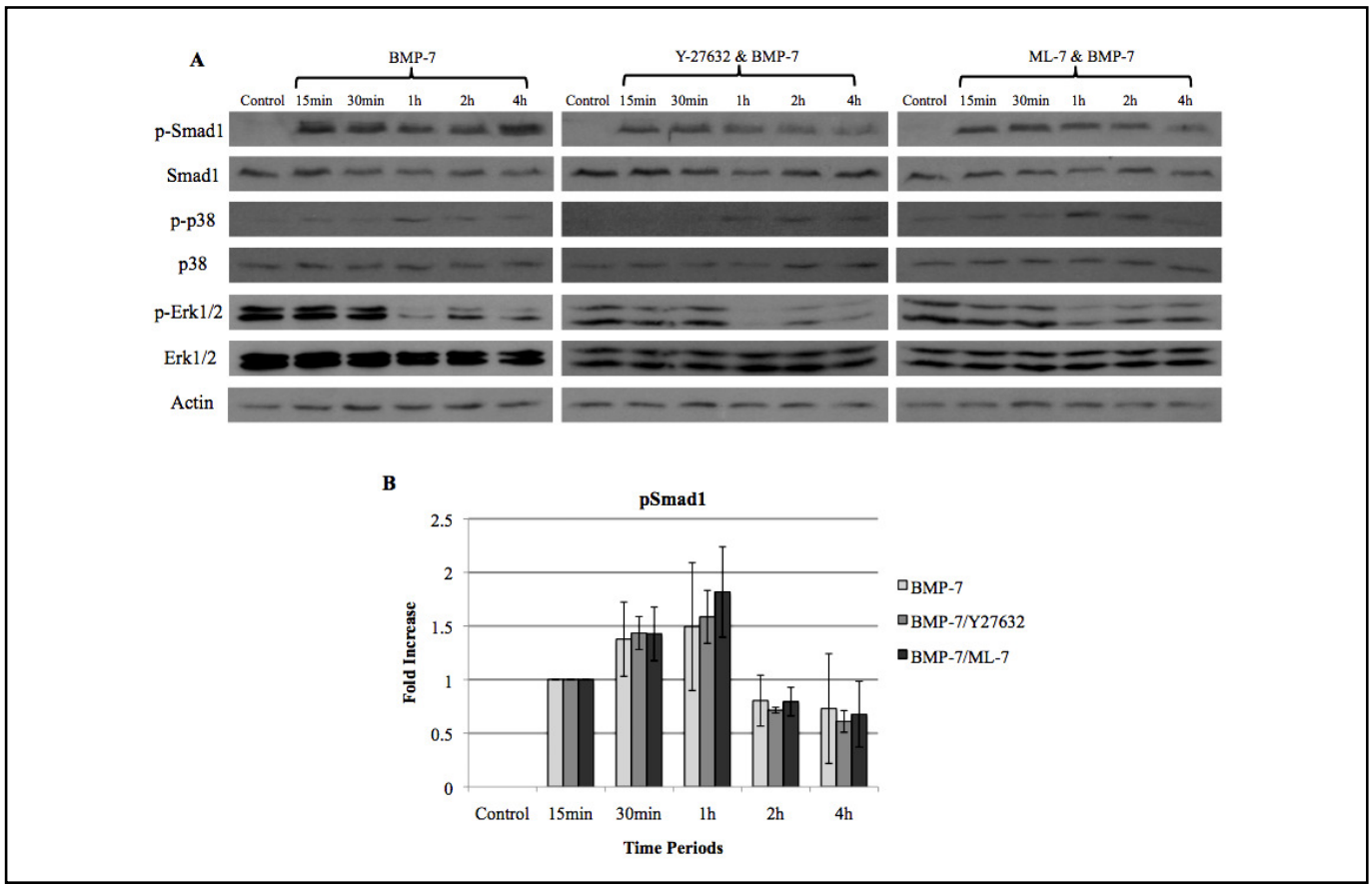

Fig. 6. The ROCK inhibitor Y-27632 and MLCK inhibitor ML-7 do not affect the BMP-7-induced phosphorylation of Smad1 and MAPK in Swiss3T3 fibroblasts. A. Representative blots are showing the amount of Smad1, p38 and p44/p42 MAPK (Erk1/2) phosphorylation from 24 h-serum-starved non-stimulated (Control) and BMP-7-stimulated (30 ng/mL) Swiss3T3 fibroblasts for the indicated time periods after pretreatment with 10 μM Y-27632 and 5 μM ML-7 for 45 min. Total protein levels for Smad1, p38, Erk1/2 and actin are also shown. B. The ratios presented in bar graphs are showing the band intensity of pSmad1 normalized to the total Smad1 of untreated or Y-27632 and ML-7-co-treated fibroblasts as mean values ± S.E. of three distinct experiments. The kinetics of Smad1 phosphorylation of untreated or Y-27632 and ML-7-co-treated fibroblasts follows the same pattern.

inhibitory effect of Y-26763 was quantified using soluble to insoluble actin immunoblotting and proved significant inhibition (Fig. 5B). The effect of the ROCK1 inhibitor against BMP-7 signaling that targets the actin cytoskeleton, is in good correlation with the effect of the same inhibitor against TGF-β1 signaling [25].

The same ROCK1 inhibitor was also potent in blocking cell migration in response to BMP-7 in the wound healing assay (Fig. 5C). There is a smaller wound closure and also additionally a lower density of migratory cells in the wound area when cells were treated with ROCK1 inhibitor. Thus, the ROCK1 activity is critical for mediating signals to actin, which can physiologically be translated to the ability of the cell to be motile.

In control experiments, we verified that the ROCK1 inhibitor did not perturb the activity of the upstream signaling by the BMP receptor, as measured by activation of phosphorylated levels of Smad1, p38 and Erk1/2 (Fig. 6). Indeed, co-treatment of cells with Y- 27632 and BMP-7 had no measurable impact on the kinetics or accumulation of C-terminally phosphorylated Smad1, or on the profiles of phospho-p38 and phospho-Erk1/2 MAPKs, as expected. We conclude that the Y-27632 inhibitor acts downstream of the Smad1 and MAPK signaling proteins and probably acts in a specific manner by limiting the activity of the ROCK1 kinase.

BMP-7 induces rapid and sustained myosin light chain phosphorylation

Signaling downstream of ROCK1 can be directed towards various kinases, including members of the PAK and LIMK families and further downstream substrates

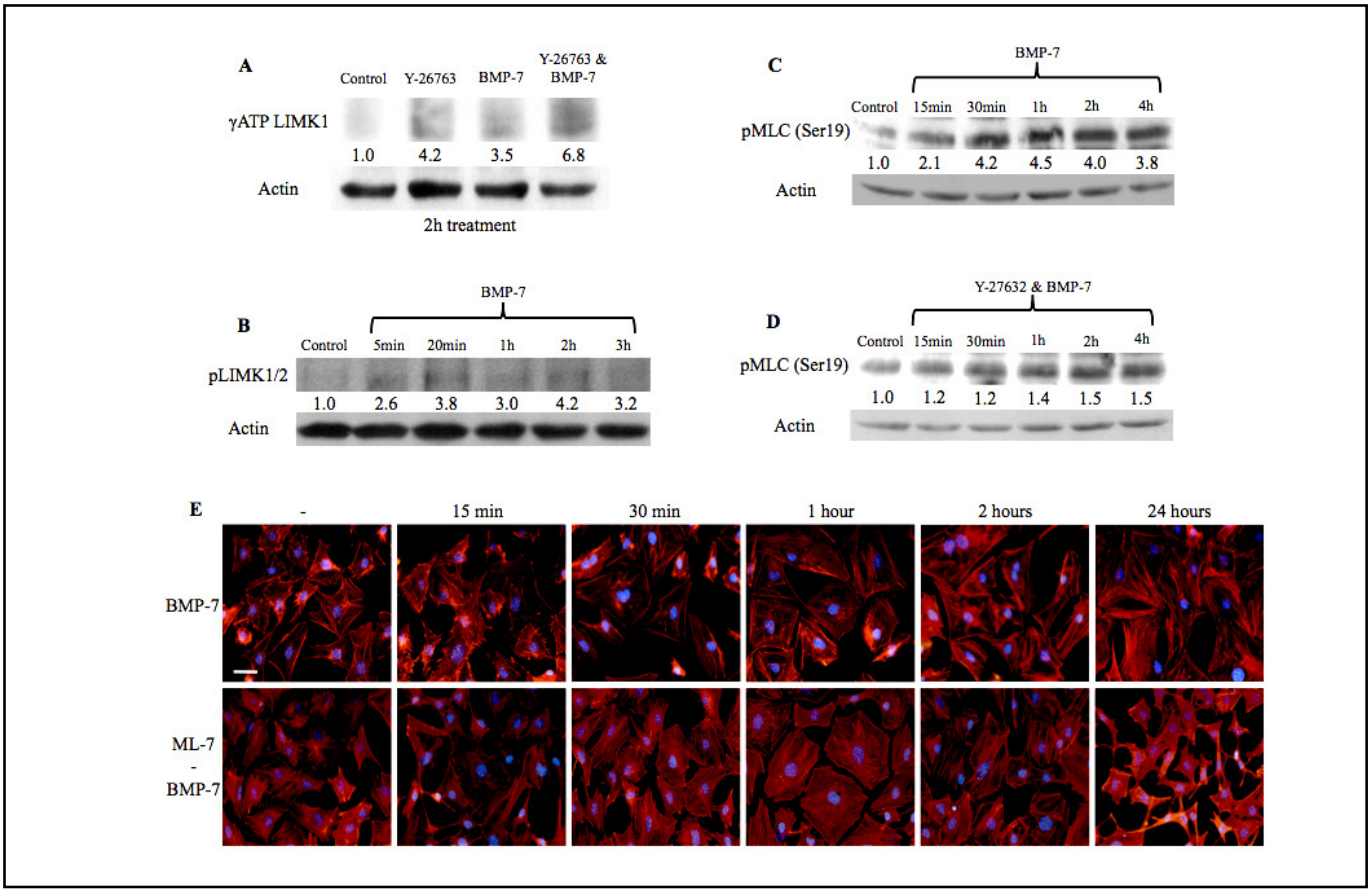

Fig. 7. BMP-7 induces rapid and sustained LIMK and MLC phosphorylation in Swiss3T3 fibroblasts. A-D. ROCK inhibitor Y-27632 unexpectedly leads to an induction of LIMK1 phosphorylation and to a dramatic reduction of BMP-7-induced MLC phosphorylation. Representative experiment showing the amount of proteins from 24 h-serum-starved non-stimulated (Control) and BMP-7-stimulated (30 ng/mL) Swiss3T3 fibroblasts for the indicated time periods. Protein levels were determined by autoradiography (A: [32P]-γATP *in vitro* kinase assay) and immunoblotting (B-D) with antibodies specific for phospho-LIMK1/2 (T508/505) and phospho-MLC (S19) (upper panels). The blots were analyzed by densitometry, and the intensity of the protein bands was normalized to the intensity of the corresponding actin band (lower panels B-D) and reported between the blots. E. MLCK inhibitor ML-7 blocks 24 h-BMP-7-mediated actin reorganization. Swiss3T3 fibroblasts serum-starved for 24 h were stimulated with 30 ng/mL BMP-7 for the indicated time periods after pretreatment with 5 μM ML-7 for 45 min. Cells were fixed and stained with rhodamine- phalloidin and DAPI. A bar represents 10 μm.

such as cofilin or MLC [5-10]. In order to rationally discriminate between these parallel signaling pathways, we made use of the ROCK1 inhibitor and theorized that for a specific pathway to be of relevance BMP-7 had to induce its activity and the ROCK1 inhibitor should block its activity. Based on the previously established critical role of LIMK1 downstream of BMP signaling in neuronal, kidney and myoblastic cells [19, 20, 24], we first tested for LIMK1 (Fig. 7A). Using an *in vitro* kinase assay with radioactive ATP and immunoprecipitates of endogenous LIMK1 from the BMP-7-stimulated cells, we could measure that BMP-7 induced a significant (3.5-fold) increase of LIMK1 phosphorylation (Fig. 7A). Unexpectedly, co-treatment of the cells with the Y-26732 inhibitor dramatically enhanced both control and BMP-7-stimulated levels of phosphorylated LIMK1 (Fig. 7A). A time-course experiment also demonstrated that phosphorylation of LIMK1 was induced rapidly and sustained for up to 3 h post-BMP-7 stimulation (Fig. 7B). These experiments reproduce the previous observations from different cell types [19, 20, 24]. However, the ability of Y-26732 to enhance LIMK1 activation by BMP-7, suggested that LIMK1 may not be the critical regulator that mediates the positive effects on the actin cytoskeleton. For the above reason, and based on failed attempts to measure significant effects

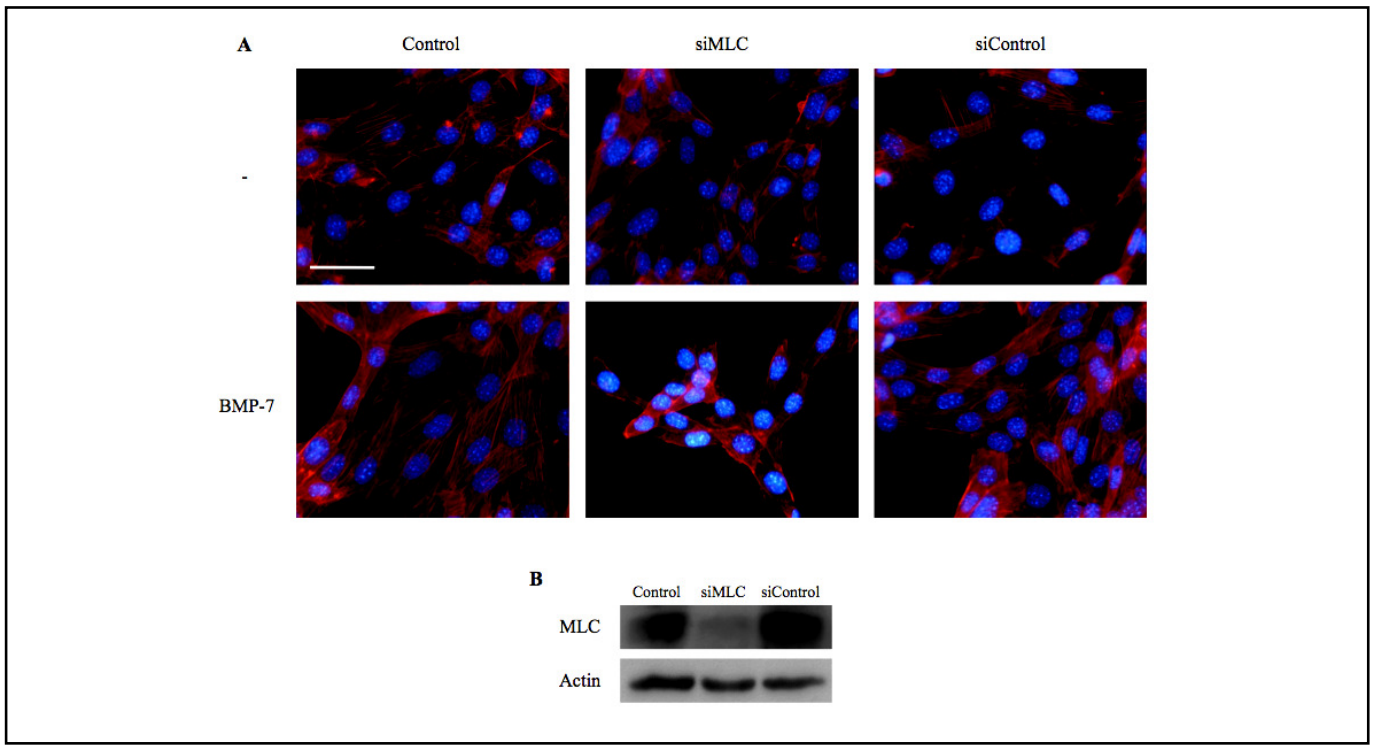

Fig. 8. Depletion of endogenous MLC using siRNA inhibits the actin reorganization induced by BMP-7. A. NIH3T3 fibroblasts were left untreated (Control) or transiently transfected with specific siMLC or negative control siRNAs for 24 h, then serum-starved for another 24 h and finally were stimulated with 30 ng/mL BMP-7 or not (-) for a final 24 h. Cells were fixed and stained with rhodamine-phalloidin and DAPI. A bar represents 10 μm. B. Corresponding immunoblot from the same cells treated as in panel A, for the MLC and control actin proteins.

on PAK family kinases (data not shown), we directed our attention on phosphorylation of MLC, an event with critical functional impact on acto-myosin remodeling associated with cell motility [10]. BMP-7 induced a rapid and time-dependent activation of phosphorylated (on Ser 19) MLC levels that sustained up to 4 h (Fig. 7C). Co-treatment of the cells with BMP-7 and Y-27632 effectively blocked the BMP-7-induced phospho-MLC levels (Fig. 7D). We therefore conclude that the BMP-7-RhoA-ROCK1 pathway may be responsible for the regulation of the MLC protein, during BMP-7-mediated actin reorganization.

Phosphorylation of MLC is a critical event during BMP-7-induced actin remodeling

In order to evaluate the functional impact of MLC phosphorylation downstream of BMP-7 we took two complementary approaches, inhibition of the kinase that phosphorylates MLC, MLC kinase (MLCK), and direct knock down of MLC using RNAi. The MLCK inhibitor ML-7 had no impact on the actin cytoskeleton integrity in control serum-starved cells (Fig. 7E). In contrast, ML-7 completely blocked the actin reorganization induced by BMP-7, which was especially evident after 24 h stimulation (Fig. 7E).

As indicated for the ROCK inhibitor, we verified in control experiments that the ML-7 inhibitor did not influence the activity of the upstream signaling by the BMP receptor, as measured by activation of phosphorylated levels of Smad1, p38 and Erk1/2 (Fig. 6). From these findings we conclude that the ML-7 inhibitor acts downstream of the Smad1 and MAPK signaling proteins and probably acts in a specific manner by limiting the activity of the MLC kinase as expected.

In a similar manner, depleting NIH3T3 cells from endogenous MLC using a specific siRNA prohibited BMP-7 from inducing effects on the actin cytoskeleton (Fig. 8A). The efficiency of knock down of endogenous MLC in these experiments was better than 85% (Fig. 8B). Under control conditions without BMP-7 stimulation, the same siRNA targeting MLC had no obvious impact on cell viability or actin cytoskeleton during the prolonged starvation applied in all these experiments (Fig. 8A). The same experiment, when performed in Swiss3T3 cells gave

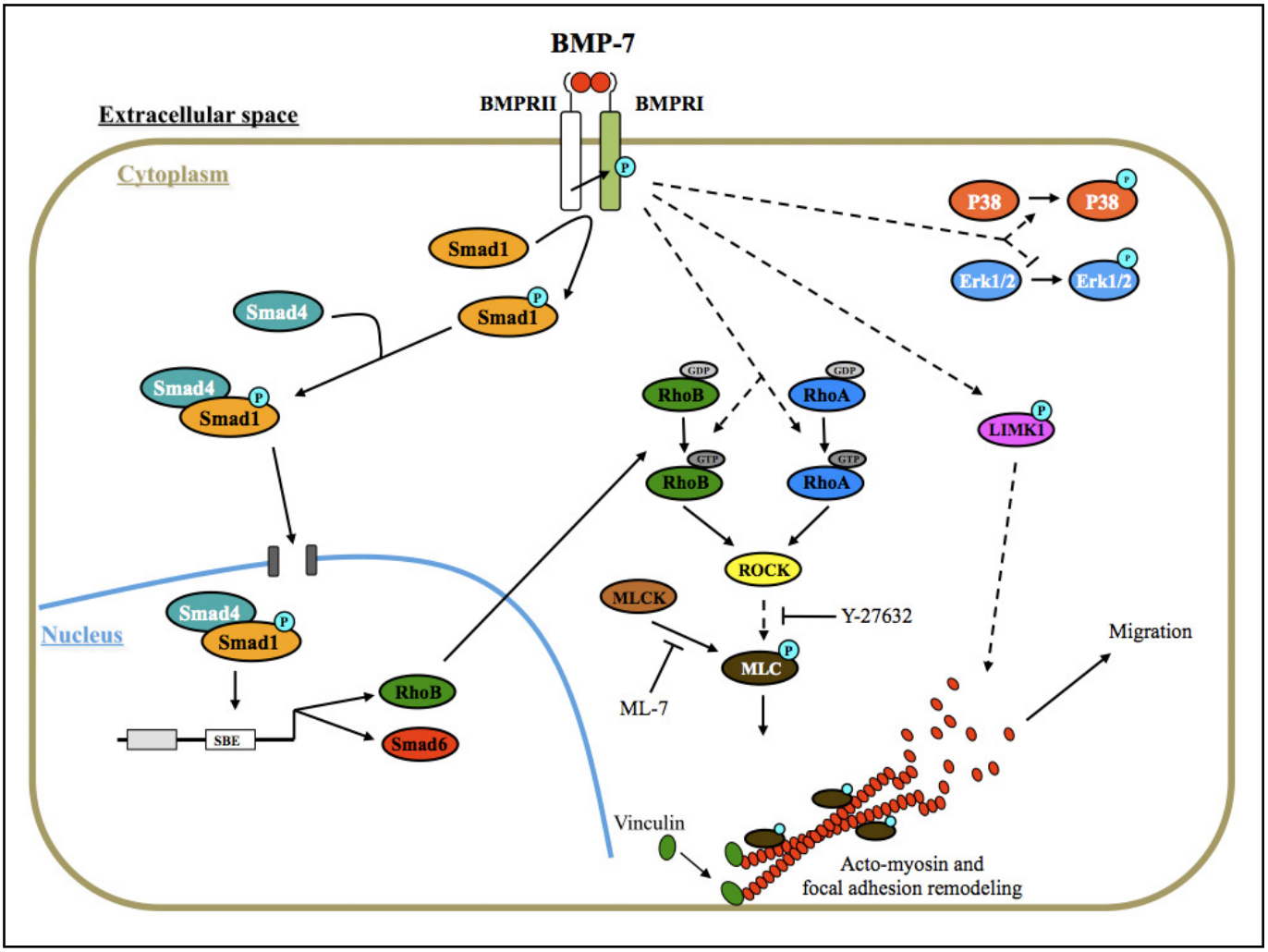

Fig. 9. Schematic representation of proposed mechanisms regulating protein phosphorylation and expression, actin cytoskeleton reorganization and migration in Swiss3T3 fibroblasts following BMP-7 stimulation. Solid arrows indicate experimentally confirmed pathways. Dotted arrows indicate experimentally verified signaling steps with unknown intermediate components. The dotted arrow leading to RhoB mRNA expression signifies the verified, albeit weak, effects of BMP-7 signaling on RhoB mRNA accumulation. The action points of the pharmacological inhibitors used are also indicated.

much weaker efficiency of knock down (less than 30%) and for this reason the NIH3T3 cell system was analyzed.

The combined experiments of MLCK inhibition and MLC siRNA convincingly establish that regulation of MLC function is a critical downstream target of BMP-7 signaling during actin remodeling.

Discussion

We present a new signaling pathway that mediates effects of a prominent member of the TGF-β family, BMP-7, on the actin cytoskeleton (Fig. 9). This pathway resembles to some extent a pathway that we previously established downstream of TGF-β1 in the same fibroblast system [25]. However, the BMP-7 pathway diverges significantly and emphasizes possible unique signaling outputs that are pathway-specific. Based on evidence where specific kinase inhibitors were combined with assays for measuring phosphorylated levels of kinases and target substrates, we propose that BMP-7 signaling via Rho GTPases and the ROCK1 kinase eventually targets the regulatory subunit of the myosin complex, MLC, functionally impacting on the assembly of the acto-myosin cytoskeleton.

Signaling by BMP receptors in regulation of actin dynamics has been examined by a few recent reports [19, 20, 24]. A common signaling intermediate established from these reports has been the kinase LIMK1, which directly phosphorylates cofilin and thus controls the

dynamic polymerization of actin. While we were able to measure activation of LIMK1 kinase activity after BMP-7 stimulation (Fig. 7A), much to our surprise, the ROCK1 inhibitor that blocks all effects of BMP-7 on the acto-myosin system and on cell motility (Fig. 5), it enhanced LIMK1 kinase activity (Fig. 7A). This result led us disqualify LIMK1 as a functionally relevant kinase that mediates cytoskeletal reorganization in response to BMP-7 in Swiss3T3 cells. However, the establishment of LIMK1 in the BMP-2 and BMP-7 pathways studied in neurons, kidney epithelial cells and myoblasts [19, 20, 24], does not all allow us to consider LIMK as a signaling mediator of lesser impact. However, it must be noted that the previous studies failed to establish a functional role of LIMK1 in cytoskeletal reorganization per se. LIMK1 was shown to be critical for dendritogenesis in cells in culture [20], while *in vivo* studies in *Xenopus* have demonstrated that LIMK1 is important for axonogenesis and not for dendritogenesis [23], introducing the complexity of functions a single protein, such as LIMK1 may exhibit in different cell types. The only direct demonstration of the role of a LIMK member downstream of a member of the TGF-β/BMP family and affecting directly actin reorganization has been for LIMK2, which mediates signals downstream of TGF-β [25]. Thus, the precise role of LIMK1 downstream of BMP receptors leading to actin remodeling requires further detailed analysis.

This study emphasizes regulation at the level of MLC phosphorylation downstream of BMP-7 (Fig. 7C). While MLC phosphorylation by MLCK is a widely established mechanism that controls the assembly of the acto-myosin filaments in muscle and non-muscle cell types [10, 31], its functional role during physiological events driven by TGF-β/BMP family signaling has not been previously addressed. Although, we did not measure directly kinase activity of MLCK downstream of BMP-7 signaling, the evidence based on the MLCK inhibitor ML-7 and the RNAi experiments targeting MLC (Fig. 7E, 8), convincingly place this kinase and its substrate MLC as functionally important regulators of acto-myosin remodeling in fibroblasts responding to BMP-7.

Based on several experiments of pharmacologic inhibition of ROCK1 kinase (Fig. 5A,C, 6D), we place for the first time ROCK1 as the upstream kinase that mediates the effects of Rho GTPase activation in response to BMP-7. ROCK1 could be equally well activated by RhoA-GTP and RhoB-GTP [3, 5], and we found both of these small GTPases activated in response to BMP-7 (Fig. 4B). However, we have not determined whether these two small GTPases play redundant roles in the process of actin reorganization. The possibility that these two small GTPases might function during distinct phases of the BMP-7 response deserves further detailed analysis. In addition, we failed to measure positive activation of Cdc42 by BMP-7 in the fibroblasts, whereas BMP-2 has been shown to induce this small GTPase in neurons and myoblasts [20, 24]. Whether the difference is based on the cell type or the specific ligand that activates the BMP receptors remains unknown.

Finally, as all previous studies primarily monitored Smad1 activation by BMP receptors during mobilization of the Rho GTPase/LIMK pathway [19, 20, 24], we also monitored the classical, so-called, non-Smad pathways of various MAPKs that are usually rapidly activated by TGF-β family receptors (Fig. 4A). In addition to C-terminally phosphorylated Smad1, BMP-7 induces rapidly phosphorylation of p38 MAPK and dephosphorylation of Erk1/2 MAPK (Fig. 4A). The impact of these kinases in mediating activation of Rho GTPases remains unexplored. In fact, this is one of the least understood steps in the cascade of signaling events that link TGF-β family receptors to the regulation of actin dynamics. In other words, we do not understand whether small GTPases of the Rho family become directly activated by the TGF-β/BMP receptors or via the Smads or any of the rapidly induced MAPKs [18]. In addition, the phospho-inositide 3'-kinase has been implicated in the regulation of the actin cytoskeleton by BMP-2 [24]. However, the mechanism by which BMP receptors activate the phospholipid kinase or by which this kinase regulates Rho GTPases downstream of BMP remains unclear. This is an important area for future investigations.

In summary, we present novel evidence that links for the first time two well-established regulators of acto-myosin assembly to the BMP pathway. One is the ROCK1 kinase acting downstream of Rho GTPases, and the other is MLCK and its substrate MLC, that regulate myosin function in the acto-myosin contractile fibril.

Acknowledgements

The work was supported by the Greek Secretariat for Research and Technology (PENED Program 03EΔ688), the Ludwig Institute for Cancer Research and the Swedish Research Council grant K2007- 66X-14936-04-3. We thank Drs. D. Kardassis and K. Sampath for valuable reagents.

References

1 Papakonstanti EA, Stournaras C: Cell responses regulated by early reorganization of actin cytoskeleton. FEBS Lett 2008;582:2120-2127.

2 Pollard TD, Cooper JA: Actin, a central player in cell shape and movement. Science 2009;326:1208-1212.

3 Heasman SJ, Ridley AJ: Mammalian rho gtpases: New insights into their functions from in vivo studies. Nat Rev Mol Cell Biol 2008;9:690-701.

4 Rossman KL, Der CJ, Sondek J: Gef means go: Turning on rho gtpases with guanine nucleotide-exchange factors. Nat Rev Mol Cell Biol 2005;6:167-180.

5 Narumiya S, Tanji M, Ishizaki T: Rho signaling, rock and mdia1, in transformation, metastasis and invasion. Cancer Metastasis Rev 2009;28:65-76.

6 Parrini MC, Matsuda M, de Gunzburg J: Spatiotemporal regulation of the pak1 kinase. Biochem Soc Trans 2005;33:646-648.

7 Bernard O: Lim kinases, regulators of actin dynamics. Int J Biochem Cell Biol 2007;39:1071-1076.

8 Oser M, Condeelis J: The cofilin activity cycle in lamellipodia and invadopodia. J Cell Biochem 2009;108:1252-1262.

9 Bernstein BW, Bamburg JR: Adf/cofilin: A functional node in cell biology. Trends Cell Biol 2010;20:187-195.

10 Takashima S: Phosphorylation of myosin regulatory light chain by myosin light chain kinase, and muscle contraction. Circ J 2009;73:208-213.

11 Moustakas A, Heldin C-H: The regulation of tgfβ signal transduction. Development 2009;136:3699-3714.

12 Gordon KJ, Blobe GC: Role of transforming growth factor-β superfamily signaling pathways in human disease. Biochim Biophys Acta 2008;1782:197-228.

13 Massagué J: Tgfβ in cancer. Cell 2008;134:215-230.

14 Miyazono K, Maeda S, Imamura T: Bmp receptor signaling: Transcriptional targets, regulation of signals, and signaling cross-talk. Cytokine Growth Factor Rev 2005;16:251-263.

15 Heldin C-H, Landström M, Moustakas A: Mechanism of tgf-β signaling to growth arrest, apoptosis, and epithelial-mesenchymal transition. Curr Opin Cell Biol 2009;21:166-176.

16 Moustakas A, Heldin C-H: Dynamic control of tgf-β signaling and its links to the cytoskeleton. FEBS Lett 2008;582:2051-2065.

17 Padua D, Massagué J: Roles of tgfβ in metastasis. Cell Res 2009;19:89-102.

18 Kardassis D, Murphy C, Fotsis T, Moustakas A, Stournaras C: Control of transforming growth factor β signal transduction by small gtpases. FEBS J 2009;276:2947-2965.

19 Foletta VC, Lim MA, Soosairajah J, Kelly AP, Stanley EG, Shannon M, He W, Das S, Massagué J, Bernard O: Direct signaling by the bmp type ii receptor via the cytoskeletal regulator limk1. J Cell Biol 2003;162:1089-1098.

20 Lee-Hoeflich ST, Causing CG, Podkowa M, Zhao X, Wrana JL, Attisano L: Activation of limk1 by binding to the bmp receptor, bmprii, regulates bmp-dependent dendritogenesis. EMBO J 2004;23:4792-4801.

21 Podkowa M, Zhao X, Chow CW, Coffey ET, Davis RJ, Attisano L: Microtubule stabilization by bone morphogenetic protein receptor-mediated scaffolding of c-jun n-terminal kinase promotes dendrite formation. Mol Cell Biol 2010;30:2241-2250.

22 Eaton BA, Davis GW: Lim kinase1 controls synaptic stability downstream of the type ii bmp receptor. Neuron 2005;47:695-708.

23 Hocking JC, Hehr CL, Bertolesi G, Funakoshi H, Nakamura T, McFarlane S: Limk1 acts downstream of bmp signaling in developing retinal ganglion cell axons but not dendrites. Dev Biol 2009;330:273-285.

24 Gamell C, Osses N, Bartrons R, Ruckle T, Camps M, Rosa JL, Ventura F: Bmp2 induction of actin cytoskeleton reorganization and cell migration requires pi3-kinase and cdc42 activity. J Cell Sci 2008;121:3960-3970.

25 Vardouli L, Moustakas A, Stournaras C: Lim-kinase 2 and cofilin phosphorylation mediate actin cytoskeleton reorganization induced by transforming growth factor-β. J Biol Chem 2005;280:11448-11457.

26 Papakonstanti EA, Stournaras C: Actin cytoskeleton architecture and signaling in osmosensing. Methods Enzymol 2007;428:227-240.

27 Vardouli L, Vasilaki E, Papadimitriou E, Kardassis D, Stournaras C: A novel mechanism of tgfβ-induced actin reorganization mediated by smad proteins and rho gtpases. FEBS J 2008;275:4074-4087.

28 Vasilaki E, Papadimitriou E, Tajadura V, Ridley AJ, Stournaras C, Kardassis D: Transcriptional regulation of the small gtpase rhob gene by tgfβ-induced signaling pathways. FASEB J 2010;24:891-905.

29 Ishida W, Hamamoto T, Kusanagi K, Yagi K, Kawabata M, Takehara K, Sampath TK, Kato M, Miyazono K: Smad6 is a smad1/5-induced smad inhibitor. Characterization of bone morphogenetic protein-responsive element in the mouse smad6 promoter. J Biol Chem 2000;275:6075-6079.

30 Katoh K, Kano Y, Amano M, Kaibuchi K, Fujiwara K: Stress fiber organization regulated by mlck and rho-kinase in cultured human fibroblasts. Am J Physiol Cell Physiol 2001;280:C1669-1679.

31 Fukata Y, Amano M, Kaibuchi K: Rho-rho-kinase pathway in smooth muscle contraction and cytoskeletal reorganization of non-muscle cells. Trends Pharmacol Sci 2001;22:32-39.